HOKKAIDO UNIVERSITY

Instructions for use

Stress Concentration Factors of Twisted Bars with L, T and Cruciform Cross-sections

Hiromasa ISHIKAWA* and Hiroshi HANZAWA*

(Received August 21, 1967)

Abstract

It is well known that stress concentration occurs at the root of a fillet of the cross-section of a twisted bar used as a structural member. Since the torsional problems of the bars having T and cruciform section have not been solved exactly, it has been assumed that the stress concentrations at the fillet of these sections are the same as for the L-section.

In this paper, by means of application of the Schwartz-Christoffels' transformation, the torsional problems of prismatical bars with L, T and cruciform sections having finite sizes are investigated. In order to calculate the stresses the digital computor (HITAC 5020) is used. For the purpose of checking the results obtained by theoretical calculation, the analogy using the conducting sheet method is employed. It is found that the theoretical calculations are in reasonable agreement with the experimental results.

Finally, the effects of the leg-length, leg -thickness and the fillet radius of these cross sections on the stress concentration are discussed.

It is concluded that the stress concentrations at the fillet of T and cruciform sections are not the same for the L-section. The stress concentrations for these sections are greatly influenced by the length and thickness of legs.

Contents

Symbols

u, v, w . . . . components of displacements in x, y and z directions respectively

---

* Department of mechanical Engineering, Faculty of Engineering.

$x,\ y,\ z$	rectangular coordinates (z sometimes means $x+iy$)
θ	angle of twist per unit length
$\varphi(x,y)$	torsion function
G	modulus of rigidity
$\psi(x,y)$	conjugate harmonic function of $\varphi(x,y)$
$F(z),\ F_1(\zeta)$	complex torsion function
$\tau_{xz},\ \tau_{yz}$	shear stress components
$f(\zeta)$	mapping function
$\pi\lambda_j$	external angle of the polygon in z-plane
L	leg-length of the cross-section
$b\ (\text{or } w)$	leg-thickness of the cross-section
ρ	radius of the fillet
Ce	stress concentration factor

1. Intrduction

It is well known that stress concentration occurs at the root of a fillet of the cross-section of a twisted bar used as a structural member. However, the only cross-section for which the stress concentrations have been obtained is the L-shaped angle-iron, especially for the case of its leg-length being large in comparison with its leg-thickness.

In this paper, the torsional problems of prismatical bars with L, T and cruciform sections having finite sizes are investigated. At first the cross-sections of the bars in the z-plane are mapped onto the unit circles in the ζ-plane by means of Schwartz-Christoffel's transformation. Then the complex torsion functions are decided using the Muskhelishvili's theory.

The digital computer (HITAC 5020) is used to represent the mapping function and the complex torsion function as the power series in ζ. The torsional stresses and the values of the stress concentration factor for L, T and cruciform sections are calculated.

For the purpose of checking the results obtained by theoretical calculation, the analogy using the conducting sheet method is employed. It is found that the theoretical calculations are in reasonable agreement with the experimental results.

2. Method of Analysis. Basic Equations

Let us consider a long prismatical bar with uniform cross-section under torsion, and fix the z-axis of the Cartesian coordinate axes to be parallel to the generators of the bar and to pass through the centroid of the cross-sections. Defining the displacement components as u, v and w in the x, y and z directions

respectively, the Saint-Venant assumptions are as follows:

$$u = -\theta y z, \quad v = \theta x z, \quad w = \theta \varphi(x, y), \tag{a}$$

where θ is an angle of twist per unit length of the bar and $\varphi(x, y)$ is a function of x and y which is called the torsion function.

The non-vanishing stresses are the shear stresses

$$\tau_{xz} = G\theta\left(\frac{\partial \varphi}{\partial x} - y\right), \quad \tau_{yz} = G\theta\left(\frac{\partial \varphi}{\partial y} + x\right), \tag{b}$$

where G is the modulus of rigidity. Substituting these stresses into the equilibrium equations, it is easily shown that these equations will be satisfied, provided that

$$\frac{\partial^2 \varphi}{\partial x^2} + \frac{\partial^2 \varphi}{\partial y^2} = 0 \tag{1}$$

Now, instead of torsion function $\varphi(x, y)$, let us introduce a function $\phi(x, y)$ which is a conjugate harmonic of and related to $\varphi(x, y)$ by the Cauchy-Riemann equations

$$\frac{\partial \varphi}{\partial x} = \frac{\partial \phi}{\partial y}, \quad \frac{\partial \varphi}{\partial y} = -\frac{\partial \phi}{\partial x} \tag{c}$$

In terms of function $\phi(x, y)$, the boundary condition is expressed as follows:

$$\phi(x, y) = \frac{1}{2}(x^2 + y^2) + c, \tag{2}$$

where c is a constant.

Hence, using the complex torsion function $F(z)$ which is defined as

$$F(z) = \varphi + i\phi, \quad z = x + iy, \tag{3}$$

the equation (b) becomes

$$\tau_{xz} - i\tau_{yz} = G\theta\left\{F'(z) - i\bar{z}\right\}, \tag{d}$$

where $\quad \bar{z} = x - iy$

In the case where the shapes of cross-section are not circular, the torsion problem may be solved by using the mapping method. Let a function $f(\zeta)$ be the mapping function which maps the region of the cross-section on to the circle $|\zeta| < 1$, and be

$$z = x + iy = f(\zeta) \tag{4}$$

Then the complex torsion function $F(z)$ is given by

$$F(z) = \varphi + i\psi = F\left[f(\zeta)\right] = F_1(\zeta) , \tag{5}$$

and $f(\zeta)$ will be holomorphic inside the bonndary.   Hence, from eqs. (3) and (4), the boundary condition becomes

$$F_1(\zeta) - \bar{F}_1(\bar{\zeta}) = if(\zeta)\bar{f}(\bar{\zeta}) + \text{const.} \tag{6}$$

Furthermore, from eq. (d), we get

$$\tau_{xz} - i\tau_{yz} = G\theta \left\{ \frac{F_1'(\zeta)}{f'(\zeta)} - i\bar{f}(\bar{\zeta}) \right\} \tag{7}$$

Therefore, we may solve the torsion problem[1] provided that the mapping function $f(\zeta)$ and the complex torsion function $F_1(\zeta)$ are obtained from eqs. (4), (6) and (7).

3.   Determination of the functions $f(\zeta)$ and $F_1(\zeta)$.

(i) In the case of L-section.

Let us consider the L-section with the leg-length $L = 1$, the leg-thickness b and fillet radius ρ, as shown in Fig. 1.

Applying the Schwarz-Christoffel transformation, a polygon region in the z-plane may be generally mapped on to the unit circle in the ζ-plane by the following relation

$$\frac{d}{d\zeta} \log \frac{dz}{d\zeta} = -\sum_j \frac{\lambda_j}{\zeta - \zeta_j} , \tag{8}$$

where $\pi\lambda_j$ is the external angle of the polygon in the z-plane.
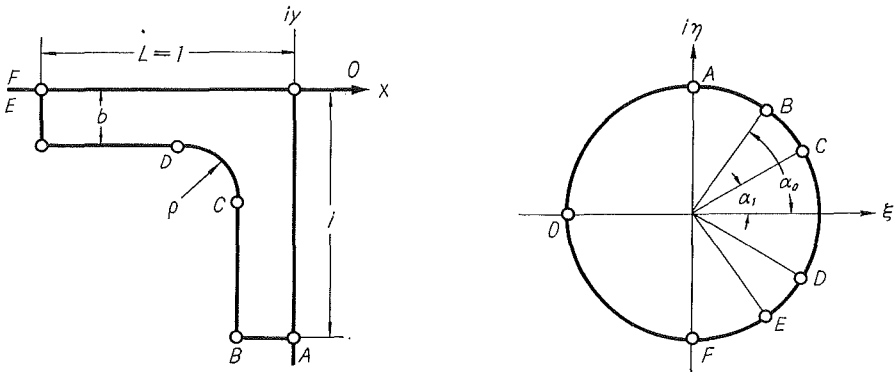

Fig. 1.

At a round corner from C to D in Fig. 1, we assume that the external angles between tangents at two consecutive points on the arc CD are given

by $\pi d\lambda_j$ and the numbers of these tangents are increased infinitely. Then the limiting form of eq. (8) becomes[2],[3]

$$\frac{d}{d\zeta}\left(\log\frac{dz}{d\zeta}\right) = -\int\frac{d\lambda_j}{\zeta-\zeta_j}\,,$$

where ζ_j indicates the point on the unit circle in the ζ-plane corresponding to the point in the z-plane at which the tangent makes an angle $\pi\lambda_j$ with some fixed line, and the integral must be taken along the curves the tangents of which are supposed to change monotonically.

Now, assuming that $\zeta_j(\lambda)$ is a function of λ such as

$$\zeta_j(\lambda) = e^{i(k\lambda+c)}\,, \tag{9}$$

where c is a constant, the points in the z-plane correspond to the points in the ζ-plane as shown in Table 1. From eq. (9) and the Table 1, we get

$$k = 4\alpha_1\,, \qquad c = -3\alpha_1$$

Thus eq. (9) becomes

$$\zeta(\lambda) = e^{i(4\alpha_1\lambda-3\alpha_1)} \tag{10}$$

and eq. (8)

$$\frac{d}{d\zeta}\log\frac{dz}{d\zeta} = -\left[\frac{\frac{1}{2}}{\zeta-i}+\frac{\frac{1}{2}}{\zeta+i}+\frac{\frac{1}{2}}{\zeta-e^{i\alpha_0}}+\frac{\frac{1}{2}}{\zeta-e^{-i\alpha_0}}\right.$$
$$\left.+\int_1^{\frac{1}{2}}\frac{d\lambda}{\zeta-e^{-3\alpha_1 i}e^{4\alpha_1\lambda i}}+\frac{\frac{1}{2}}{\zeta+1}\right] \tag{11}$$

TABLE 1

z-plane	ζ-plane
A (z_A)	$\zeta_A = e^{\frac{\pi}{2}} = i$
B (z_B)	$\zeta_B = e^{i\alpha_0}$
C (z_C)	$\zeta_C = e^{i\alpha_1} = e^{i(k+c)}$
D (z_D)	$\zeta_D = e^{-i\alpha_1} = e^{i\left(\frac{k}{2}+c\right)}$
E (z_E)	$\zeta_E = e^{-i\alpha_0}$
F (z_F)	$\zeta_F = e^{-\frac{\pi}{2}i} = -i$
O (z_G)	$\zeta_O = e^{\pi i} = -1$

The integral on the right-hand side of eq. (11) is

$$\int_1^{\frac{1}{2}} \frac{d\lambda}{\zeta - e^{-3\alpha_1 i}e^{4\alpha_1 \lambda i}} = \frac{1}{4\alpha_1 i\zeta}\left[\log(1 - e^{-\alpha_1 i}\zeta) - \log(1 - e^{\alpha_1 i}\zeta)\right]$$

$$= \frac{1}{4i\alpha_1 \zeta}\sum_{n=1}^{\infty}\frac{1}{n}\left\{(-1)^{n-1}(-e^{-i\alpha_1}\zeta)^n - (-1)^{n-1}(-e^{i\alpha_1}\zeta)^n\right\}$$

$$= \frac{1}{4i\alpha_1}\sum_{n=1}^{\infty}\frac{1}{n}\left\{e^{in\alpha_1} - e^{-in\alpha_1}\right\}\zeta^{n-1} = \sum_{n=1}^{\infty}\frac{a'_n}{n}\zeta^{n-1},$$

where $\quad a'_n = \dfrac{1}{2\alpha_1}\sin n\alpha_1$.

Then eq. (11) becomes

$$\frac{d}{d\zeta}\log\frac{dz}{d\zeta} = -\left[\frac{\frac{1}{2}}{\zeta - i} + \frac{\frac{1}{2}}{\zeta + i} + \frac{\frac{1}{2}}{\zeta - e^{i\alpha_0}} + \frac{\frac{1}{2}}{\zeta - e^{-i\alpha_0}}\right.$$

$$\left. + \sum_{n=1}^{\infty}\frac{a'_n}{n}\zeta^{n-1} + \frac{\frac{1}{2}}{\zeta + 1}\right],$$

and integrating the above eq., we can obtain

$$\frac{dz}{d\zeta} = c_1 \exp\left[-\frac{1}{2}\left\{\log(1 + i\zeta) + \log(1 - i\zeta) + \log(1 - e^{-i\alpha_0}\zeta)\right.\right.$$

$$\left.\left. + \log(1 - e^{i\alpha_0}\zeta) + \log(1 + \zeta)\right\} - \sum_{n=1}^{\infty}\frac{a'_n}{n}\zeta^n\right]$$

$$= c_1 \exp\left(\sum_{n=1}^{\infty}a_n\zeta^n - \sum_{n=1}^{\infty}\frac{a'_n}{n^2}\zeta^n\right) \tag{12}$$

where $\quad a_n = -\dfrac{1}{2n}\left[(-1)^{n-1}\left\{1 + (-1)^n\right\}i^n + (-1)^{n-1} - 2\cos n\alpha_0\right]$

Therefore, we get

$$a_n = \begin{cases} \dfrac{1}{2n}(2\cos n\alpha_0 - 1) & (n = \text{odd}) \\[2mm] \dfrac{1}{2n}(2\cos n\alpha_0 + 2i^n + 1) & (n = \text{even}) \end{cases}$$

Furthermore, if we write

$$\sum_{n=1}^{\infty}a_n\zeta^n - \sum_{n=1}^{\infty}\frac{a'_n}{n^2}\zeta^n = \sum_{n=1}^{\infty}A_n\zeta^n, \tag{13}$$

then

$$A_n = \begin{cases} \dfrac{1}{2n}\left(2\cos n\alpha_0 - 1\right) - \dfrac{1}{n^2}\cdot\dfrac{\sin n\alpha_1}{2\alpha_1} & (n = \text{odd}) \\[3mm] \dfrac{1}{2n}\left(2\cos n\alpha_0 + 2i^n + 1\right) - \dfrac{1}{n^2}\cdot\dfrac{\sin n\alpha_1}{2\alpha} & (n = \text{even}) \end{cases} \tag{14}$$

If the exponential function in eq. (12) is expanded in the form of a power series of ζ, we get

$$\frac{dz}{d\zeta} = c_1 \exp\left(\sum_{n=1}^{\infty} A_n \zeta^n\right) = c_1 \sum_{n=1}^{\infty} b_n \zeta^n \tag{15}$$

where $b_0 = 1$ and b_n are functions of the coefficients $A_1, A_2, \cdots A_n$.

Integrating eq. (15) with respect to ζ, we get

$$z = c_1 \sum_{n=1}^{\infty} \frac{b_n}{n+1} \zeta^{n+1} + c_2 \tag{16}$$

Thus the mapping function is represented in a power series of ζ.

Now, let us determine the coefficients c_1 and c_2. If we define $t_n = \dfrac{b}{n+1}$, eq. (16) becomes

$$z = c_1(\zeta + t_1\zeta + t_2\zeta^3 + \cdots) + c_2 \tag{17}$$

Noting that $z=-i$ corresponds to $\zeta=i$ and $z=-1$ to $\zeta=-i$, and $z=0$ to $\zeta=-1$, we get

$$c_1 = -\frac{1+i}{2}\cdot\frac{1}{CKE} \quad \text{and} \quad c_2 = c_1 W,$$

where $\quad CKE = 1 + (-1)^{\frac{2}{2}} t_2 + (-1)^{\frac{4}{2}} t_4 + (-1)^{\frac{6}{2}} t_6 + \cdots$

$$W = 1 + (-1)^1 t_1 + (-1)^2 t_2 + (-1)^3 t_3 + \cdots$$

Substituting eq. (17) into eq. (6) and expanding the function in a power series in $\zeta(n=10)$, we can obtain the complex torsion function as

$$\begin{aligned} F_1(\zeta) = {}& ic_1\bar{c}_2\left\{\zeta + t_1\zeta^2 + t_2\zeta^3 + t_3\zeta^4 + \cdots t_{10}\zeta^{11}\right\} \\ & + ic_1{}^{\varkappa}{}_1\Big[(t_{10}\bar{t}_9 + t_9\bar{t}_8 + t_8\bar{t}_7 + t_7\bar{t}_6 + \cdots + t_2\bar{t}_1 + t_2)\zeta^2 \\ & \qquad + (t_{10}\bar{t}_8 + t_9\bar{t}_7 + t_8\bar{t}_6 + \cdots + t_3\bar{t}_1 + t_2)\zeta^2 \\ & \qquad + \cdots + (t_{10}\bar{t}_1 + t_9)\zeta^9 + t_{10}\zeta^{10}\Big] \end{aligned} \tag{18}$$

And the first derivatives of $f(\zeta)$ and $F_1(\zeta)$ with respect to ζ are

$$z' = f'(\zeta) = c_1 \left\{ 1 + b_1\zeta + b_2\zeta^2 + b_3\zeta^3 + \cdots + b_{10}\zeta^{10} \right\} \tag{19}$$

$$F_1'(\zeta) = ic_1\bar{c}_1 \left[10\, t_{10}\zeta^9 + 9\left(t_{10}\bar{t}_1 + t_9\right)\zeta^8 + 8\left(t_{10}\bar{t}_2 + t_9\bar{t}_1 + t_8\right)\zeta^7 \right.$$
$$\left. + \cdots + \left(t_{10}\bar{t}_9 + t_9\bar{t}_8 + t_8\bar{t}_7 + \cdots + t_2\bar{t}_1 + t_1\right) \right]$$
$$+ ic_1\bar{c}_2 \left\{ 1 + b_1\zeta + b_2\zeta^2 + b_3\zeta^3 + \cdots + b_{10}\zeta^{10} \right\} \tag{20}$$

Since the convergence of the power series in ζ into which the function $e^{\sum\limits_{n=1}^{\infty} A_n\zeta^n}$ is expanded is not good, it is required to take many terms in this series. The method of expansion is also complicated.

The program developed for the digital computer (HITAC 5020) may be used for solving other boundary-value problems by means of the same mapping function. Some of the programs are shown in Table 2 and 3. The latter shows a part of the program to calculate the coefficients of ζ in eqs. (18) and (20). These programs can be used for the next two cases of **T** and cruciform cross-sections.

(ii) In the case of T-section.

Let us consider the **T**-section with the leg-length of $L=1$, the leg-thickness of b and w, and the fillet radius of ρ as shown in Fig. 2.

Let the points O, A, B,$\cdots$, A$'$ in the z-plane correspond to the points in the ζ-plane respectively, as shown in Fig. 2 and Table 4, we get

TABLE 2.

```
     ALK=1.0
     DO 30 L=1,100
     IF(L.GT.15)GO TO 25
     ALK=ALK*FLOAT(L)
     B(L)=A(1)**L/ALK
     GO TO 30
  25 B(L)=0.0
  30 CONTINUE
     DO 40 I=2,100
     ANK=1.0
     DO 50 N=1,100
     IF(N.GT.15)GO TO 55
     ANK=ANK*FLOAT(N)
     G(N)=A(I)**N/ANK
     GO TO 65
  55 G(N)=0.0
  65 S(N)=0.0
     DO 60 M=1,N
     NIM=N-I*M
     IF(NIM.GT.0)GO TO 70
     IF(NIM.LT.0)GO TO 60
     S(N)=S(N)+G(M)
     GO TO 60
  70 S(N)=S(N)+B(NIM)*G(M)
  60 CONTINUE
     C(N)=B(N)+S(N)
  50 CONTINUE
     DO 80 J=1,100
     B(J)=C(J)
  80 CONTINUE
  40 CONTINUE
```

TABLE 3.

```
      DO 120 MM=1,100
      ST(MM)=FLOAT(MM)*T(MM)
      MMM=100-MM
      IF(MMM.EQ.0)GO TO 110
      DO 130 NN=1,MMM
      MMNN=MM+NN
      ST(MM)=ST(MM)+FLOAT(MM)*T(MMNN)*T(NN)
  130 CONTINUE
  120 CONTINUE
```
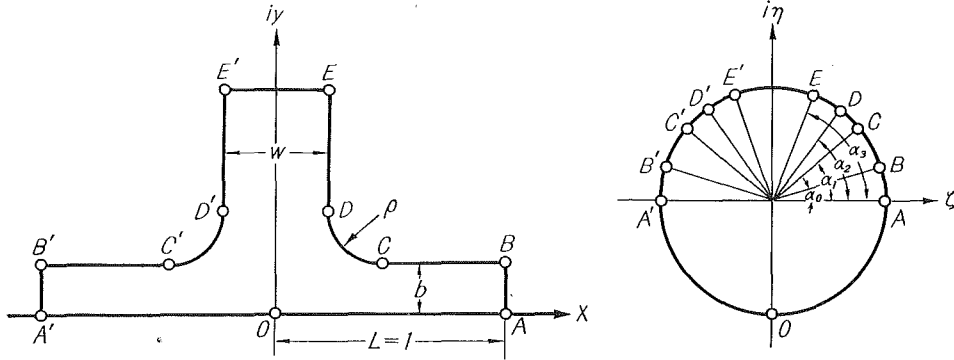
Fig. 2.

$$k = 2(\alpha_1 - \alpha_2), \quad c = 2\alpha_2 - \alpha_1, \qquad \text{(on the 1st quadrant of } \zeta\text{-plane)} \quad (21)$$

$$k = 2(\alpha_1 - \alpha_2) \quad c = \pi - 3\alpha_1 + 2\alpha_2, \quad \text{(on the 2nd quadrant of } \zeta\text{-plane)} \quad (22)$$

Therefore, eq. (18) may be reduced to the following form

$$\frac{d}{d\zeta} \log \frac{dz}{d\zeta} = -\left[\frac{\frac{1}{2}}{\zeta - 1} + \frac{\frac{1}{2}}{\zeta - e^{i\alpha_0}} + \int_{\frac{3}{2}}^{1} \frac{d\lambda}{\zeta - \zeta_2(\lambda)} + \frac{\frac{1}{2}}{\zeta - e^{i\alpha_3}} \right.$$

$$\left. + \frac{\frac{1}{2}}{\zeta + e^{-i\alpha_3}} + \frac{\frac{1}{2}}{\zeta + e^{-i\alpha_0}} + \frac{\frac{1}{2}}{\zeta + 1} + \int_{1}^{\frac{1}{2}} \frac{d\lambda}{\zeta - \zeta_1(\lambda)} \right], \quad (23)$$

where

$$\left. \begin{aligned} \zeta_1(\lambda) &= e^{i(2\alpha_2 - \alpha_1)} e^{2i\lambda(\alpha_1 - \alpha_2)} \\ \zeta_2(\lambda) &= -e^{-i(3\alpha_1 - 2\alpha_2)} e^{2i\lambda(\alpha_1 - \alpha_2)} \end{aligned} \right\} \qquad (24)$$

The integrals on the right-hand side of eq. (23) become

$$\int_{\frac{3}{2}}^{1} \frac{d\lambda}{\zeta - \zeta_2(\lambda)} + \int_{1}^{\frac{1}{2}} \frac{d\lambda}{\zeta - \zeta_1(\lambda)} = \frac{1}{2i(\alpha_1 - \alpha_2)} \left\{ -2i(\alpha_1 - \alpha_2) - \log(\zeta - e^{i\alpha_2}) \right.$$

$$\left. + \log(\zeta - e^{i\alpha_1}) - \log(\zeta + e^{-i\alpha_1}) + \log(\zeta + e^{-i\alpha_2}) \right\}$$

$$= \frac{1}{2i(\alpha_1 - \alpha_2)} \sum_{n=1}^{\infty} \frac{1}{n} \left\{ (-1)^{n-1} e^{in\alpha_2} - e^{-in\alpha_1} + e^{-in\alpha_2} - (-1)^{n-1} e^{in\alpha_1} \right\} \zeta^{n-1}$$

$$= \sum_{n=1}^{\infty} \frac{a'_n}{n} \zeta^{n-1}, \qquad (25)$$

where

$$a_n' = \begin{cases} \dfrac{i\,(\cos n\alpha_1 - \cos n\alpha_2)}{\alpha_1 - \alpha_2} & (n = \text{odd}) \\[3mm] \dfrac{\sin n\alpha_1 - \sin n\alpha_2}{\alpha_1 - \alpha_2} & (n = \text{even}) \end{cases} \qquad (26)$$

Then eq. (23) becomes

$$\frac{d}{d\zeta} \log \frac{dz}{d\zeta} = -\left[\frac{\frac{1}{2}}{\zeta - 1} + \frac{\frac{1}{2}}{\zeta + 1} + \frac{\frac{1}{2}}{\zeta - e^{i\alpha_0}} + \frac{\frac{1}{2}}{\zeta + e^{-i\alpha_0}} \right.$$

$$\left. + \frac{\frac{1}{2}}{\zeta - e^{i\alpha_3}} + \frac{\frac{1}{2}}{\zeta - e^{-i\alpha_3}} + \sum_{n=1}^{\infty} \frac{a_n'}{n} \zeta^{n-1} \right]$$

Integrating the above eq., we get

$$\frac{dz}{d\zeta} = \bar{c}_1 \exp\left[-\frac{1}{2} \left\{ \log(\zeta - 1) + \log(\zeta + 1) + \log(\zeta - e^{i\alpha_0}) + \log(\zeta + e^{-i\alpha_0}) \right.\right.$$

$$\left.\left. + \log(\zeta - e^{i\alpha_3}) + \log(\zeta - e^{-i\alpha_3}) \right\} - \sum_{n=1}^{\infty} \frac{a_n'}{n} \zeta^n \right]$$

$$= i c_1 \exp\left\{ \sum_{n=1}^{\infty} a_n \zeta^n - \sum_{n=1}^{\infty} \frac{a_n'}{n} \zeta^n \right\} , \qquad (27)$$

TABLE 4.

z-plane	ζ-plane
$A(z_A)$	$\zeta_A = e^0 = 1$
$B(z_B)$	$\zeta_B = e^{i\alpha_0}$
$C(z_C)$	$\zeta_C = e^{i\alpha_1} = e^{i(k+c)}$
$D(z_D)$	$\zeta_D = e^{i\alpha_2} = e^{i\left(\frac{k}{2}+c\right)}$
$E(z_E)$	$\zeta_{\underline{\ }} = e^{i\alpha_3}$
$E'(z_{E'})$	$\zeta_{E'} = e^{i(\pi - \alpha_3)} = -e^{-i\alpha_3}$
$D'(z_{D'})$	$\zeta_{D'} = e^{i(\pi - \alpha_2)} = -e^{-i\alpha_2} = e^{i\left(\frac{3}{2}k+c\right)}$
$C'(z_{C'})$	$\zeta'_C = e^{i(\pi - \alpha_1)} = -e^{-i\alpha_1} = e^{i(k+c)}$
$B'(z_{B'})$	$\zeta_{B'} = e^{i(\pi - \alpha_0)} = e^{--i\alpha_0}$
$A'(z_{A'})$	$\zeta_{\vartriangleleft'} = e^{i\pi} = -1$

where $\quad a_n = \begin{cases} -\dfrac{i(\sin n\alpha_0 + \sin n\alpha_3)}{n} & (n = \text{odd}) \\[2mm] \dfrac{1 + \cos n\alpha_0 + \cos n\alpha_3}{n} & (n = \text{even}) \end{cases}$

If we rewrite eq. (27) as

$$\frac{dz}{d\zeta} = ic_1 \exp\left(\sum_{n=1}^{\infty} A_n\zeta^n\right), \tag{28}$$

then

$$A_n = \begin{cases} -\dfrac{i(\sin n\alpha_0 + \sin n\alpha_3)}{n} - \dfrac{i(\cos n\alpha_1 - \cos n\alpha_2)}{(\alpha_1 - \alpha_2)n^2} & (n = \text{odd}) \\[3mm] \dfrac{1 + \cos n\alpha_0 + \cos n\alpha_3}{n} - \dfrac{\sin n\alpha_1 - \sin n\alpha_2}{(\alpha_1 - \alpha_2)n^2} & (n = \text{even}) \end{cases} \tag{29}$$

Furthermore, if we expand the function $\exp\left(\sum_{n=1}^{\infty} A_n\zeta^n\right)$ into the power series in ζ, we obtain

$$\frac{dz}{d\zeta} = ic_1 \sum_{n=1}^{\infty} b_n\zeta^n, \tag{30}$$

where $b_0 \equiv 1$, and b_n are the functions of the coefficients $A_1, A_2, \cdots A_n$. Then, integrating eq. (30) with respect to ζ, we can obtain

$$z = ic_1 \sum_{n=0}^{\infty} \frac{b_n}{n+1} \zeta^{n+1} + c_2 \tag{31}$$

Thus the mapping function may be represented in series in ζ.

By the similar procedure as the former case, we can determine the coefficients c_1 and c_2. Using the same notation $t_n = \dfrac{b_n}{n+1}$ as before, and noting that $z=1$ corresponds to $\zeta=1$, $z=-1$ to $\zeta=-1$, and $z=0$ to $\zeta=-i$, we can obtain

$$c_1 = -\frac{i}{CKE}, \quad c_2 = -c_1 W,$$

$$CKE = 1 + t_2 + t_4 + t_6 + \cdots,$$
$$W = 1 + (-i)t_1 + (-i)^2 t_3 + (-i)^2 t_3 + \cdots.$$

Finally, the conformal mapping function $z = f(\zeta)$ and the complex torsion function $F_1(\zeta)$ may be obtained as follows:

$$z = ic_1(\zeta + t_1\zeta^2 + t_2\zeta^3 + \cdots + t_{10}\zeta^{11}) + c_2$$

$$F_1(\zeta) = ic_1\bar{c}_1\left\{t_{10}\zeta^{10} + (t_{10}\bar{t}_1 + t_9)\zeta^9 + \cdots + (t_{10}\bar{t}_9 + t_9\bar{t}_8 + \cdots + t_2\bar{t}_1 + t_1)\zeta\right\}$$

$$- c_1\bar{c}_2(t_{10}\zeta^{11} + t_9\zeta^{10} + \cdots + t_1\zeta^2 + \zeta)$$

(iii) In the case of cruciform section.

Let us consider the cruciform section with the leg-length of $L=1$, the leg-thickness of b and the fillet radius of ρ as shown in Fig. 3.
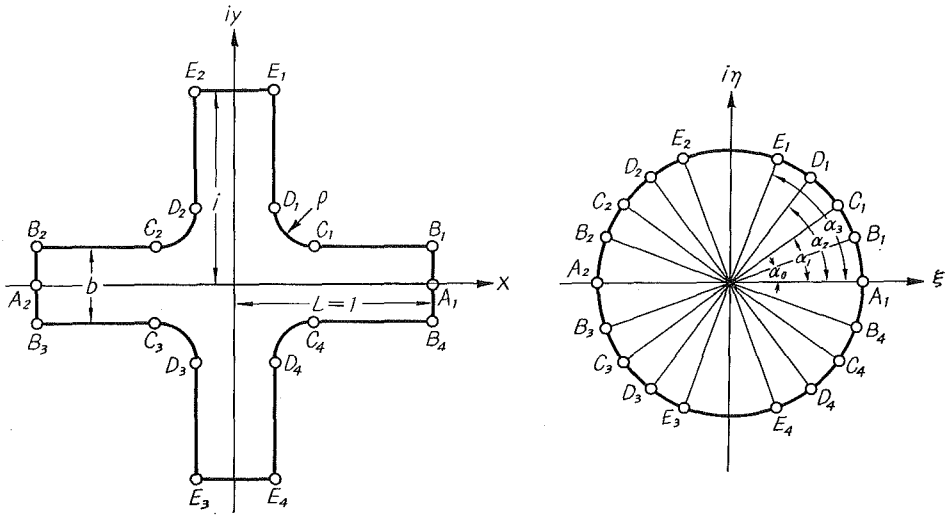

Fig. 3.

The points in the z-plane correspond to the points in the ζ-plane as shown in Table 5. Then we can obtain

$$k = 2(\alpha_1 - \alpha_2), \quad c = 2\alpha_2 - \alpha_1 \qquad \text{(on the 1st quadrant of the } \zeta\text{-plane)}$$
$$k = 2(\alpha_1 - \alpha_2), \quad c = \pi + 2\alpha_2 - 3\alpha_1 \quad \text{(on the 2nd quadrant of the } \zeta\text{-plane)}$$
$$k = 2(\alpha_1 - \alpha_2), \quad c = \pi + 2\alpha_2 - \alpha_1 \quad \text{(on the 3rd quadrant of the } \zeta\text{-plane)}$$
$$k = 2(\alpha_1 - \alpha_2), \quad c = 2\alpha_2 - 3\alpha_1 \qquad \text{(on the 4th quadrant of the } \zeta\text{-plane)}$$

and

$$\frac{d}{d\zeta}\log\frac{dz}{d\zeta} = -\left[\frac{\frac{1}{2}}{\zeta - e^{i\alpha_0}} + \int_1^{\frac{3}{2}}\frac{d\lambda}{\zeta - \zeta_1(\lambda)} + \frac{\frac{1}{2}}{\zeta - e^{i\alpha_3}} + \frac{\frac{1}{2}}{\zeta + e^{-i\alpha_3}}\right.$$

$$+ \int_{\frac{3}{2}}^1\frac{d\lambda}{\zeta - \zeta_2(\lambda)} + \frac{\frac{1}{2}}{\zeta + e^{-i\alpha_0}} + \frac{\frac{1}{2}}{\zeta + e^{i\alpha_0}} + \int_1^{\frac{3}{2}}\frac{d\lambda}{\zeta - \zeta_3(\lambda)}$$

$$+ \frac{\frac{1}{2}}{\zeta + e^{i\alpha_3}} + \frac{\frac{1}{2}}{\zeta - e^{-i\alpha_3}} + \int_{\frac{3}{2}}^{1} \frac{d\lambda}{\zeta - \zeta_4(\lambda)} + \frac{\frac{1}{2}}{\zeta - e^{-i\alpha_0}} \Bigg], \quad (32)$$

where

$$\zeta_1(\lambda) = e^{i(2\alpha_2 - \alpha_1)} e^{2i\lambda(\alpha_1 - \alpha_2)}, \qquad \zeta_3(\lambda) = -e^{i(2\alpha_2 - \alpha_1)} e^{2i\lambda(\alpha_1 - \alpha_2)}$$
$$\zeta_2(\lambda) = -e^{i(2\alpha_2 - 3\alpha_1)} e^{2i\lambda(\alpha_1 - \alpha_2)}, \quad \zeta_4(\lambda) = e^{i(2\alpha_2 - 3\alpha_1)} e^{2i\lambda(\alpha_1 - \alpha_2)} \qquad \Bigg\} \qquad (33)$$

TABLE 5.

z-plane	ζplane
z_{A_1}	$\zeta_{A_1} = e^0 = 1$
z_{B_1}	$\zeta_{B_1} = e^{i\alpha_0}$
z_{C_1}	$\zeta_{C_1} = e^{i\alpha_1} = e^{i(k+c)}$
z_{D_1}	$\zeta_{D_1} = e^{i\alpha_2} = e^{i\left(\frac{k}{2}+c\right)}$
z_{E_1}	$\zeta_{E_1} = e^{i\alpha_3}$
z_{E_2}	$\zeta_{E_2} = e^{i(\pi - \alpha_3)} = -e^{-i\alpha_3}$
z_{D_2}	$\zeta_{D_2} = e^{i(\pi - \alpha_2)} = -e^{-i\alpha_2} = e^{i\left(\frac{3}{2}k + c\right)}$
z_{C_2}	$\zeta_{C_2} = e^{i(\pi - \alpha_1)} = -e^{-i\alpha_1} = e^{i(k+c)}$
z_{B_2}	$\zeta_{B_2} = e^{i(\pi - \alpha_0)} = -e^{-i\alpha_0}$
z_{A_2}	$\zeta_{A_2} = e^{i\pi} = -1$
z_{B_3}	$\zeta_{B_3} = e^{i(\pi + \alpha_0)} = -e^{i\alpha_0}$
z_{C_3}	$\zeta_{C_3} = e^{i(\pi + \alpha_1)} = -e^{i\alpha_1} = e^{i(k+c)}$
z_{D_3}	$\zeta_{D_3} = e^{i(\pi + \alpha_2)} = -e^{i\alpha_2} = e^{i\left(\frac{k}{2}+c\right)}$
z_{E_3}	$\zeta_{E_3} = e^{i(\pi + \alpha_3)} = -e^{i\alpha_3}$
z_{E_4}	$\zeta_{E_4} = e^{-i\alpha_3}$
z_{D_4}	$\zeta_{D_4} = e^{-i\alpha_2} = e^{i\left(\frac{3}{2}k + c\right)}$
z_{C_4}	$\zeta_{C_4} = e^{-i\alpha_1} = e^{i(k+c)}$
z_{B_4}	$\zeta_{B_4} = e^{-i\alpha_0}$

The integrals on the right-hand side of eq. (32) are

$$\int_{1}^{\frac{1}{2}} \frac{d\lambda}{\zeta - e^{i(2\alpha_2 - \alpha_1)} e^{2i\lambda(\alpha_1 - \alpha_2)}} + \int_{\frac{3}{2}}^{1} \frac{d\lambda}{\zeta + e^{i(2\alpha_2 - 3\alpha_1)} e^{2i\lambda(\alpha_1 - \alpha_2)}}$$

$$+ \int_1^{\frac{1}{2}} \frac{d\lambda}{\zeta + e^{i(2\alpha_2 - \alpha_1)} e^{2i\lambda(\alpha_1 - \alpha_2)}} + \int_{\frac{3}{2}}^1 \frac{d\lambda}{\zeta - e^{i(2\alpha_2 - 3\alpha_1)} e^{2i\lambda(\alpha_1 - \alpha_2)}}$$

$$= \frac{1}{2i(\alpha_1 - \alpha_2)\zeta} \left\{ -4i(\alpha_1 - \alpha_2) - \log(\zeta - e^{i\alpha_2}) + \log(\zeta - e^{i\alpha_1}) \right.$$

$$- \log(\zeta + e^{-i\alpha_1}) + \log(\zeta + e^{-i\alpha_2}) - \log(\zeta + e^{i\alpha_2})$$

$$\left. + \log(\zeta + e^{i\alpha_1}) - \log(\zeta - e^{-i\alpha_1}) + \log(\zeta - e^{-i\alpha_2}) \right\}$$

$$= \frac{1}{2i(\alpha_1 - \alpha_2)\zeta} \left\{ \log(1 - e^{-i\alpha_1}\zeta) + \log(1 + e^{-i\alpha_1}\zeta) + \log(1 + e^{i\alpha_2}\zeta) \right.$$

$$+ \log(1 - e^{i\alpha_2}\zeta) - \log(1 - e^{i\alpha_1}\zeta) - \log(1 + e^{i\alpha_1}\zeta)$$

$$\left. - \log(1 + e^{-i\alpha_2}\zeta) - \log(1 - e^{-i\alpha_2}\zeta) \right\}$$

$$= \frac{1}{2i(\alpha_1 - \alpha_2)} \sum_{n=1}^\infty \frac{1}{n} \left[\left\{ (-1)^{n-1} - 1 \right\} e^{-in\alpha_1} + \left\{ (-1)^{n-1} - 1 \right\} e^{in\alpha_2} \right.$$

$$\left. + \left\{ 1 - (-1)^{n-1} \right\} e^{in\alpha_1} + \left\{ 1 - (-1)^{n-1} \right\} e^{-in\alpha_2} \right] \zeta^{n-1}$$

$$= \sum_{n=1}^\infty \frac{1}{n} a_n' \zeta^{n-1}, \tag{34}$$

where

$$a_n' = \begin{cases} 0 & (n = \text{odd}) \\ \dfrac{2(\sin n\alpha_1 - \sin n\alpha_2)}{\alpha_1 - \alpha_2} & (n = \text{even}) \end{cases}$$

Then eq. (32) becomes

$$\frac{d}{d\zeta} \log \frac{dz}{d\zeta} = - \left[\frac{\frac{1}{2}}{\zeta - e^{i\alpha_0}} + \frac{\frac{1}{2}}{\zeta + e^{i\alpha_0}} + \frac{\frac{1}{2}}{\zeta + e^{-i\alpha_0}} + \frac{\frac{1}{2}}{\zeta - e^{-i\alpha_0}} + \frac{\frac{1}{2}}{\zeta - e^{i\alpha_3}} \right.$$

$$\left. + \frac{\frac{1}{2}}{\zeta + e^{i\alpha_3}} + \frac{\frac{1}{2}}{\zeta + e^{-i\alpha_3}} + \frac{\frac{1}{2}}{\zeta - e^{-i\alpha_3}} + \sum_{n=1}^\infty \frac{a_n'}{n} \zeta^{n-1} \right]$$

Integrating the above eq., we obtain

$$\frac{dz}{d\zeta} = c_1 \exp \left[-\frac{1}{2} \left\{ \log(\zeta - e^{i\alpha_0}) + \log(\zeta + e^{i\alpha_0}) + \log(\zeta + e^{-i\alpha_0}) \right. \right.$$

$$+ \log(\zeta - e^{-i\alpha_0}) + \log(\zeta - e^{i\alpha_3}) + \log(\zeta + e^{i\alpha_3})$$

$$\left. \left. + \log(\zeta + e^{-i\alpha_3}) + \log(\zeta - e^{-i\alpha_3}) \right\} - \sum_{n=1}^\infty \frac{a_n'}{n^2} \zeta^n \right]$$

$$= c_1 \exp \left[\sum_{n=1}^\infty \frac{1}{2n} \left\{ 1 - (-1)^{n-1} \right\} (e^{in\alpha_0} + e^{-in\alpha_0} + e^{in\alpha_3} + e^{-in\alpha_3}) \zeta^n - \sum_{n=1}^\infty \frac{a_n'}{n} \zeta^n \right]$$

$$= c_1 \exp\left(\sum_{n=1}^{\infty} a_n \zeta^n - \sum_{n=1}^{\infty} \frac{a_n'}{n^2} \zeta^n \right), \tag{35}$$

where
$$a_n = \begin{cases} 0 & (n = \text{odd}) \\ \dfrac{2(\cos n\alpha_0 + \cos n\alpha_3)}{n} & (n = \text{even}) \end{cases}$$

If we write

$$\frac{dz}{d\zeta} = c_1 \exp\left(\sum_{n=1}^{\infty} A_n \zeta^n \right), \tag{36}$$

then

$$A_n = \begin{cases} 0 & (n = \text{odd}) \\ \dfrac{2(\cos n\alpha_0 + \cos n\alpha_3)}{n} - \dfrac{2(\sin n\alpha_1 - \sin n\alpha_2)}{(\alpha_1 - \alpha_2)n^2} & (n = \text{even}) \end{cases} \tag{37}$$

Expanding the function $\exp\left(\sum_{n=1}^{\infty} A_n \zeta^n \right)$ in eq. (36) into a power series in ζ, we can obtain

$$\frac{dz}{d\zeta} = c_1 \exp\left(\sum_{n=1}^{\infty} A_n \zeta^n \right) = c_1 \sum_{n=1}^{\infty} b_n \zeta^n$$

Since this is the same form as for **L**-section, i. e. eq. (15), the mapping function $z = f(\zeta)$ and the complex torsion function $F_1(\zeta)$ have the same forms as eqs. (16) and (18).

Noting that $z = 0$ corresponds to $\zeta = 0$, $z = 1$ to $\zeta = 1$ and $z = -1$ to $\zeta = -1$, we can obtain

$$c_2 = 0 \quad \text{and} \quad c_1 = \frac{1}{CKE},$$

where $CKE = 1 + t_2 + t_4 + t_6 + \cdots$.

Therefore we can determine the mapping function and the complex torsion function.

4.   Results of the Theoretical Calculation.

(i) **In the case of L-section.**

The thickness b and fillet radius ρ of the legs are determined by eqs. (14) ane (16), using the assumed values of angle α_0 and α_1.   At first we consider

the case of $\alpha_0 = 87°$, $\alpha_1 = 30°$.

Numerical calculations are performed using 100 terms in the power series of ζ.   Table 6 shows the calculated results of the co-ordinates of the points in the z-plane and the resultant shear stresses at the points corresponding to the points (α) on the unit circle $\zeta = e^{i\alpha}$ in the ζ-plane.

TABLE 6.   (**L**) $\alpha_0 = 87°$, $\alpha_1 = 30°$

	α	$0°$	$30°$	$45°$	$60°$	$75°$	$85°$
co-ordinates	x	-0.470	-0.459	-0.459	-0.459	-0.459	-0.465
	y	-0.470	$-0,497$	-0.526	-0.574	-0.672	-0.867
resultant shear stress	$\tau/G\theta$	2.088	1.259	0.567	0.442	0.436	0.333

	α	$87°$	$89°$	$90°$	$120°$	$150°$	$180°$
	x	-0.409	-0.151	-0.034	0.017	0.017	0.000
	y	-1.035	-1.105	-1.034	-0.476	-0.299	0.000
	$\tau/G\theta$	0.277	0.281	0.279	0.484	0.457	0.152

In this Table only 12 points are shown, but the calculation was performed for 30 points.   The locations of these points and the magnitudes of the stresses at these points are plotted in Fig. 4 as white and black circles, respectively.

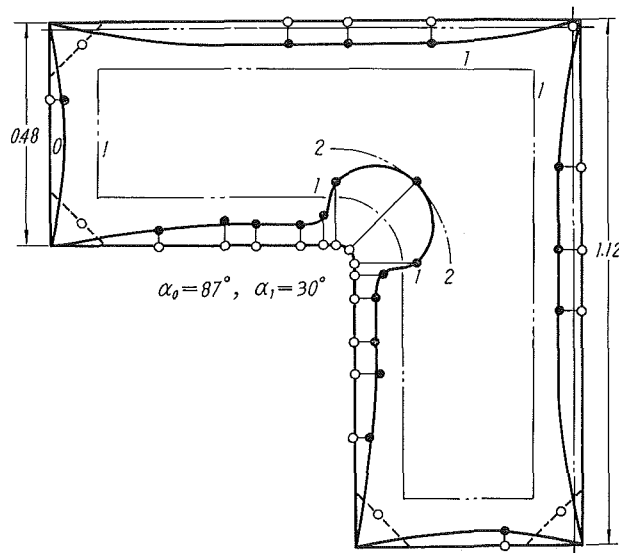From the result of this calculation, one can notice some discrepancies with
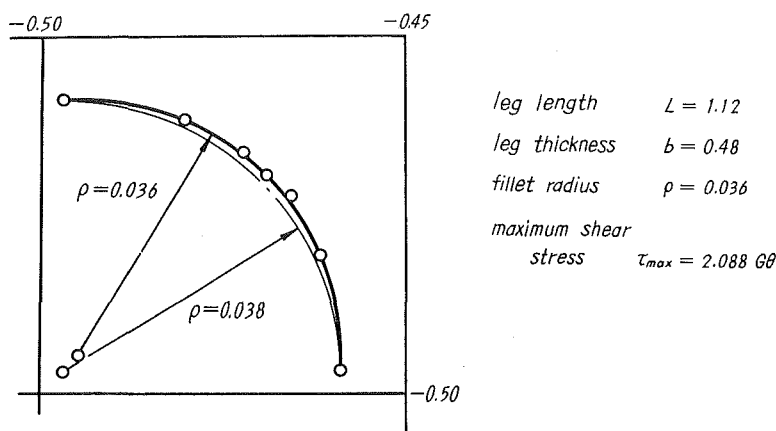

Fig. 4. (L)

leg length $L = 1.12$

leg thickness $b = 0.48$

fillet radius $\rho = 0.036$

maximum shear
    stress $\tau_{max} = 2.088\ G\theta$

Fig. 5.

the assumed condition.   The convex corners of the legs (A, B, E, F) are not sharp and have some roundness.   Fig. 5 shows an enlarged figure of the concave corner $\overparen{CD}$.   The radius of curvature estimated from the curve drawn by the thick line which is traced along the points obtained by calculation is 0.036, and the radius determined from a quarter circular arc drawn by the fine line through the two points C and D is 0.038.   The latter is larger by 5.3% than the former.   The calculated leg-length is larger by 12% than the assumed length of $L=1$.   Furthermore, since the values of x corresponding to $\alpha=120°$ and 150° in Table 6 must be zero, the results are larger by 1.7% than the correct values.   The reason for this is probally that the finite number of terms used in the power series in ζ was not sufficient to obtain exact values.

Table 7 shows the corresponding co-ordinates x, y and the resultant shear stresses for the case of $\alpha_0=80°$ and $\alpha_1=30°$.   These are plotted in Fig. 6.

TABLE 7.   (**L**) $\alpha_0=80°$, $\alpha_1=30°$

	α	0°	30°	45°	60°	75°	80°
co-ordinates	x	−0.544	−0.530	−0.531	−0.531	−0.532	−0.499
	y	−0.544	−0.579	−0.616	−0.682	−0.833	−1.018
resultant shear stress	$\tau/G\theta$	1.611	1.071	0.654	0.512	0.380	0.227

	α	85°	90°	105°	120°	150°	180°
	x	−0.263	−0.015	0.019	0.019	0.019	0.000
	y	−1.056	−1.015	−0.659	−0.529	−0.335	0.000
	$\tau/G\theta$	0.337	0.237	0.515	0.552	0.520	0.171

$\alpha_0 = 80°, \quad \alpha_1 = 30$

leg length $L = 1.08$
leg thickness $b = 0.55$
fillet radius $\rho = 0.05$
maximum shear
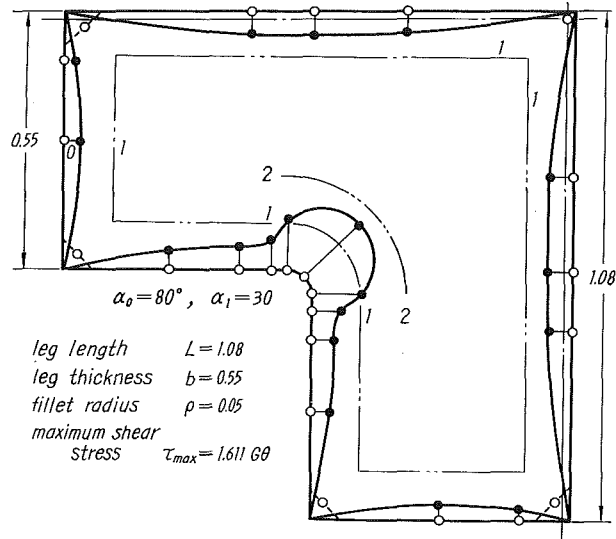   stress $\tau_{max} = 1.611 \, G\theta$

Fig. 6. (L)

The convex corners of the legs are also not sharp, but their errors are smaller than for the former case. The leg-length is 8% longer than the assumed length $(L=1)$. But the radius of the fillet determined by tracing the points coincides with the radius determined by C and D.

(ii) In the case of T-section.

In this case, the thicknesses of the horizontal and vertical legs are determined by the values of angle α_0 and α_3, respectively, and the fillet radius is determined by the angles α_1 and α_2.

The numerical calculations are performed by taking 100 terms in the power series in ζ for both case of $\alpha_0 = 3°$, $\alpha_1 = 30°$, $\alpha_2 = 60°$, $\alpha_3 = 87°$, and $\alpha_0 = 10°$, $\alpha_1 =$

TABLE 8.　(**T**)　$\alpha_0 = 3°$, $\alpha_1 = 30°$, $\alpha_2 = 60°$, $\alpha_3 = 87°$

		0°	3°	8°	15°	30°	45°
co-ordinates	x	1.000	1.000	0.646	0.500	0.367	0.317
	y	0.069	0.576	0.646	0.646	0.646	0.662
resultant shear stress	$\tau/G\theta$	0.378	0.378	0.528	0.628	0.857	1.818

		60°	87°	90°	270°	200°	330°
	x	0.299	0.255	0.000	0.000	0.122	0.287
	y	0.709	1.219	1.256	0.000	0.000	0.000
	$\tau/G\theta$	1.078	0.294	0.653	0.717	0.759	0.654

$\alpha_0 = 3°$, $\alpha_1 = 30°$
$\alpha_2 = 60°$, $\alpha_3 = 87°$

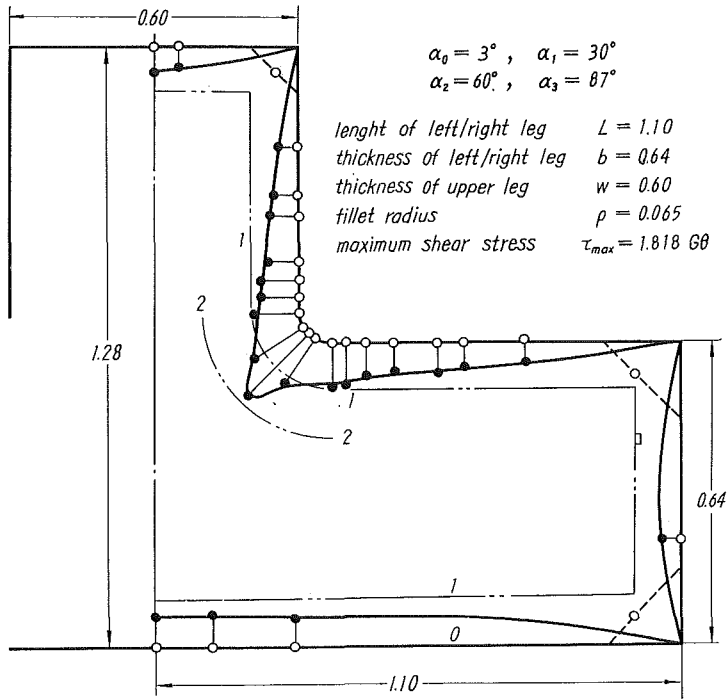| lenght of left/right leg | $L = 1.10$ |
thickness of left/right leg	$b = 0.64$
thickness of upper leg	$w = 0.60$
fillet radius	$\rho = 0.065$
maximum shear stress	$\tau_{max} = 1.818\ G\theta$

Fig. 7.   (T)

$30°$, $\alpha_2 = 60°$, $\alpha_3 = 80°$.

Table 8 and Fig. 7 show the co-ordinates of x and y, and the resultant shear stresses for the case of the former set of α_n.   The convex corners of the legs are also not sharp, but the fillet radius determined by tracing the points coincides with the radius determined by the points C and D.   The length of the left (and right legs) is larger by 10% than the assumed length ($L = 1$).

TABLE 9.   (T) $\alpha_0 = 10°$, $\alpha_1 = 30°$, $\alpha_2 = 60°$, $\alpha_3 = 80°$

	α	0°	10°	15°	20°	30°	45°
co-ordinates	x	1.000	1.000	0.724	0.615	0.501	0.429
	y	0.049	0.761	0.811	0.807	0.809	0.835
resultant shear stress	$\tau/G\theta$	0.350	0.346	0.596	0.875	1.085	1.928

	α	60°	80°	90°	270°	300°	330°
	x	0.403	0.370	0.000	0.000	0.146	0.340
	y	0.903	1.303	1.335	0.000	0.000	0.000
	$\tau/G\theta$	1.237	0.290	0.795	0.913	0.918	0.829

$$\alpha_0 = 10°, \quad \alpha_1 = 30°$$
$$\alpha_2 = 60°, \quad \alpha_3 = 80°$$

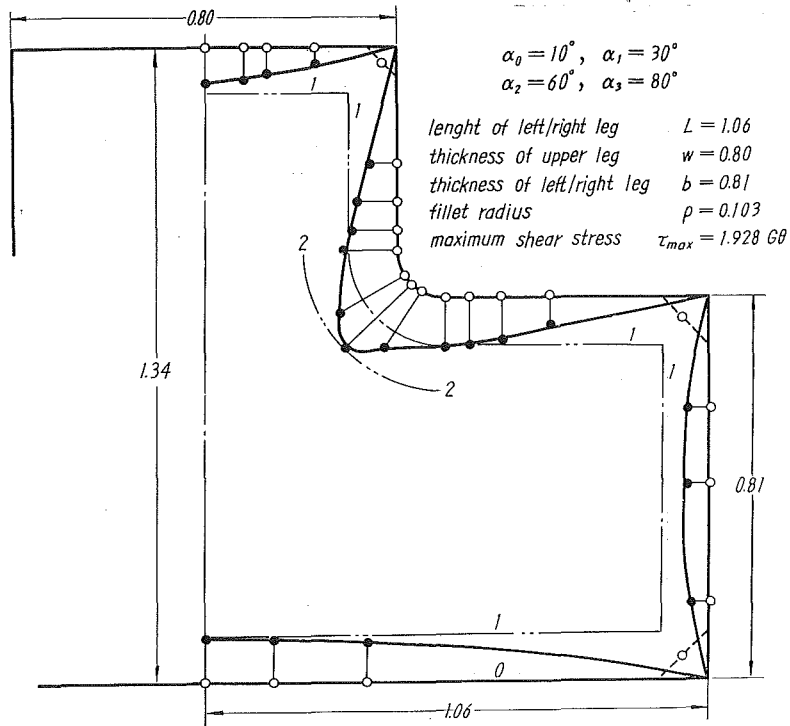|	
lenght of left/right leg	$L = 1.06$
thickness of upper leg	$w = 0.80$
thickness of left/right leg	$b = 0.81$
fillet radius	$\rho = 0.103$
maximum shear stress	$\tau_{max} = 1.928 \, G\theta$

Fig. 8. (T)

Table 9 and Fig. 8 show the case of the latter set of α_n. The convex corners of the legs are slightly improved over the former ones. The leg-length is longer by 6% than the assumed length ($L=1$). The corners of the vertical leg have less roundness than those of the left or (right) legs for both sets of α_n.

TABLE 10. (+) $\alpha_0 = 3°$, $\alpha_1 = 40°$, $\alpha_2 = 50°$, $\alpha_3 = 87°$

	α	0°	3°	10°	15°	20°	30°
co-ordinates	x	1.000	0.959	0.617	0.528	0.469	0.390
	y	0.000	0.284	0.332	0.333	0.332	0.332
resultant shear stress	τ/G	0.741	0.327	0.694	0.705	0.866	1.121

	α	45°	60°	70°	75°	87°	90°
	x	0.336	0.332	0.332	0.333	0.273	−0.006
	y	0.336	0.391	0.470	0.530	0.971	1.000
	$\tau/G\theta$	2.455	1.118	0.872	0.695	0.327	0.728

(iii) In the case of cruciform-section.

In this case, the thickness of the horizontal (left or right) leg is determined by the value of the angle α_0 and that of the vertical leg is determined by the value of angle α_3, and the fillet radius is determined by α_1 and α_2. The numerical calculations are performed by taking 100 terms in the series for the two cases $\alpha_0 = 3°$, $\alpha_1 = 40°$, $\alpha_2 = 50°$, $\alpha_3 = 87°$, and $\alpha_0 = 15°$, $\alpha_1 = 30°$, $\alpha_2 = 60°$,

$\alpha_0 = 3°$, $\alpha_1 = 40°$

$\alpha_2 = 50°$, $\alpha_3 = 87°$

length of upper/down and left/right leg $L = 1.00$

thickness of upper/down and left/right leg $b = 0.66$

fillet radius $\rho = 0.013$

maximum shear stress $\tau_{max} = 2.455 \ G\theta$
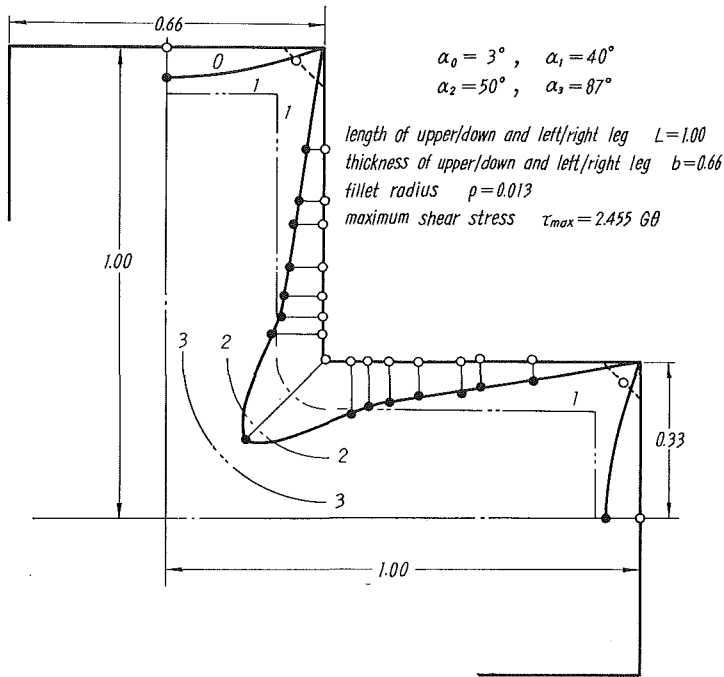
Fig. 9. (+)

TABLE 11. (+) $\alpha_0 = 15°$, $\alpha_1 = 30°$, $\alpha_2 = 60°$, $\alpha_3 = 75°$

	α	0°	10°	15°	20°	30°	40°
co-ordinates	x	1.000	1.001	0.964	0.755	0.611	0.545
	y	0.000	0.230	0.459	0.492	0.491	0.507
resultant shear stress	$\tau/G\theta$	0.785	0.645	0.324	0.676	1.190	1.662

	α	45°	50°	60°	75°	80°	90°
	x	0.523	0.507	0.491	0.451	0.226	−0.003
	y	0.523	0.545	0.612	0.971	1.001	1.000
	$\tau/G\theta$	2.438	1.660	1.180	0.324	0.650	0.787

$\alpha_0 = 15°$, $\alpha_1 = 30°$
$\alpha_2 = 60°$, $\alpha_3 = 75°$
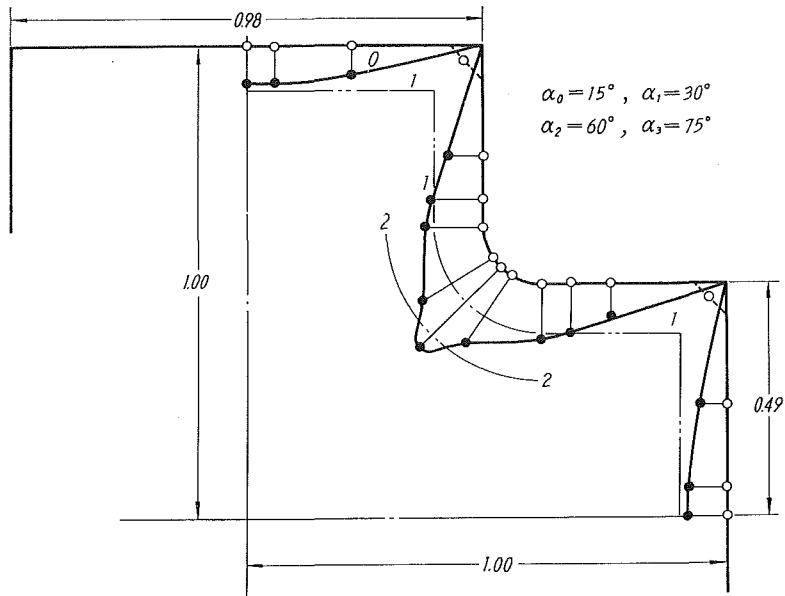
length of upper/down and left/right leg $L = 1.00$
thickness of upper/down and left/right leg $b = 0.98$
fillet radius $\rho = 0.12$
maximum shear stress $\tau_{max} = 2.438\ G\theta$

Fig. 10. (+)

$\alpha_3 = 75°$.   Table 10 and Fig. 9, and Table 11 and Fig. 10 show the co-ordinates of the points and the resultant shear stresses for the former and latter case, respectively.

In both cases, the convex corners of the legs have a slight roundness, but in the latter case it is smaller than in the former case.

5. Experimental Results.—Conducting Sheet Analogy.[4]

For the purpose of ascertaining the numerical results, the analogous experiments are performed by using a conducting sheet.

The torsional stress distribution has been measured by means of the soap-film analogy.   Recently, the technique employing the oblique incidence method of three-dimensional photo-elasticity has been developed to solve the torsion problem.   However, in these methods it is more difficult to prepare the suitable apparatus or specimens than in the following method, which uses the electric conducting sheet analogy.

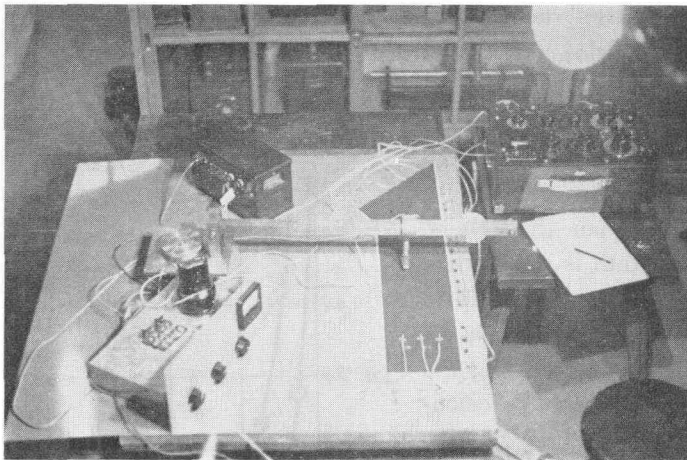In order to obtain uniform electric resistance, "anacon-paper" (similar

Fig. 11.

to the facsimile paper) was used.   Its electric resistance is 260 ohm/square. Keeping the voltage constant along the peripheries of the sheet and feeding the distributed current into it, we measured the voltages at many points on the paper.   In order to feed the electric current into the paper and keep the voltage constant, we used the highly conducting silver-paint (Dupont No. 4817) to attach the leading wire on the sheet.   Fig. 11 shows the testing apparatus and the sheet.   The experiments were done only for L/b of 2.00, i. e., the ratio of leg-length (L) to leg-thickness (b) is equal to 2.00, in three cases of **L**, **T** and cruciform sections.

6. Discussion of the Results.

The torsional shear stresses for **L**, **T** and **+**-sections having finite leg-length (L), various thicknesses (b and w), and ardii (ρ) of fillet, are calculated for some sets of angles α_0, α_1, α_2, and α_3.

Now we define the stress-concentration factor as $Ce = \tau_{\max}/bG\theta$[5)(6)(7)(8], where $bG\theta$ is the stress in a thin rectangular section.   However, it seems to be inadequate to use the above definition as a stress-concentration factor when the leg-length is not so large in comparison with its thickness and when there exists only a short portion of constant thickness at the leg.   Hence, this stress-concentration factor defined as above is used only for comparison with the results obtained by Huth[6], Beadle and Conway[9].

(i) **L-section.**

Fig. 12 shows the values of the stress-concentration factor for various ratios of fillet radius (ρ) to leg-thickness b and for three values of the angle

α_0, 87°, 85°, and 80°, which correspond to the ratios of L/b of 2.33, 2.26 and 1.97 respectively. The stress-concentration factors for both cases of $\alpha_0 = 87°$ and 85° are almost the same, but for $\alpha_0 = 80°$ it is lower than the others. The result by Huth is also shown in Fig. 12 for the ratio ρ/b up to 0.5 merely for the pursose of comparison ; because, utilizing the relaxation method, Huth calculated the value of the stress-concentration factor for ρ/b of about 0 through 2.0; also in his case the leg-length is quite long in comparison with the leg-thickness. His result coincides with the authors' one only for the ratio L/b of about 2.0.

For the ratio ρ/b up to 0.5, the larger the ratio L/b, the higher the concentration factor. And the smaller the ratio L/b becomes, the

Fig. 12. (L)

more rapidly Ce approaches to a constant value. These show that both the ratios L/b and ρ/b have a significant influence upon the stress-concentration.

The experimental results for the ratio L/b of 2.0 are also shown in Fig. 12 and we can see that the calculated and experimental results agree satisfactorily for ρ/b of about 0 through to 0.5.

(ii) **T-section.**

Fig. 13 shows the calculated values of the stress-concentration factor for various ratios of ρ/b and for three cases of the ratio of L/b (1.31, 1.72, and 1.92). The setting angles are as follows:

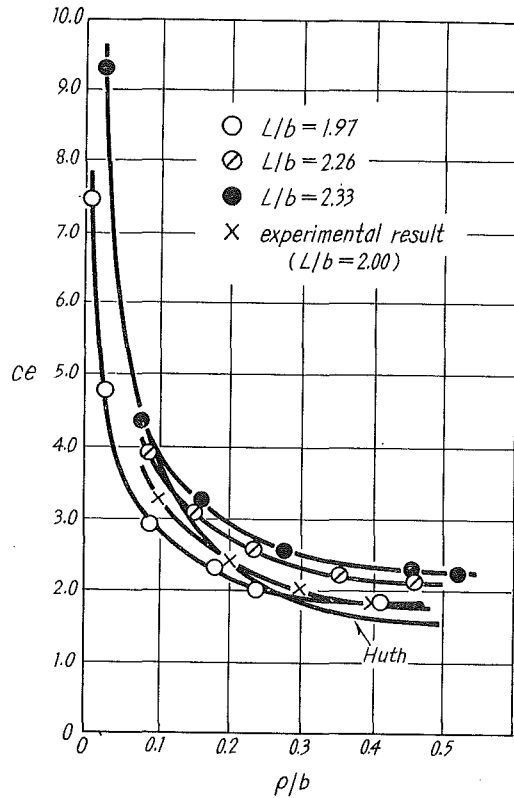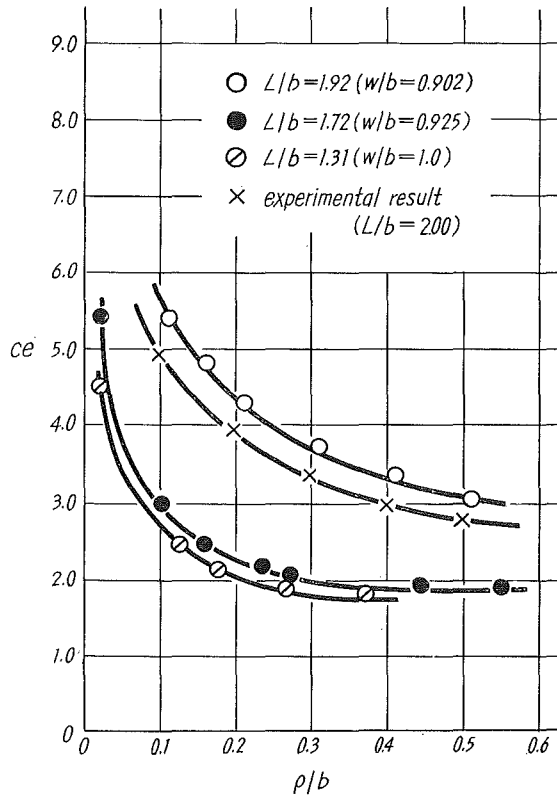| α_0	α_1							α_2	α_3	L/b	w/b
10°	15°	20°	25°	30°	40°			$90° - \alpha_1$	80°	1.31	1.0
3°	5°	10°	15°	20°	25°	30°	40°	,,	87°	1.72	0.925
1°	5°	10°	15°	20°	25°	30°		,,	89°	1.92	0.902

Fig. 13. (T)

Very little work has been done on the stress-concentration for the case of the T-section in either fields of theoretical or experimental investigations. As far as the authors know, there is only one reference in the literature. Utilizing the point-matching method, Beadle and Conway receutly calculated the stress-concentration factor for this kind of section where the leg-length is quite large in comparison with its thickness. In their case, the ratios ρ/b were more than 0.5 and the ratios w/b were 0.67 and 2.0. Therefore, the author's results can not be compared with theirs.

For the large leg-thickness ($L/b=1.72$ and 1.31) in the authors' results, the stress-concentration factor are nearly the same and approaches the constant value at the comparatively small value of ρ/b as is shown in Fig. 13. With a fixed value of $L/b=1.5$, for the cases of ρ/b about 0.5 through 1.0 and $w/b=1.0$, there is only a small zone when the leg has a constant thickness. Furthermore, with increase of the leg-thickness, the configuration of the T-

section approaches the rectangular or square section due to the constant value of w/b.

For the case of the ratio $L/b = 1.92$, the ratios ρ/b have a more distinct influence on the value of the stress-concentration foctor. The experimental results for the ratio L/b of 2.0 are also shown in Fig. 13.

(iii) +-section.

Fig. 14 shows the stress-concentration factor for various ratios of ρ/b with three values of the ratio of L/b.
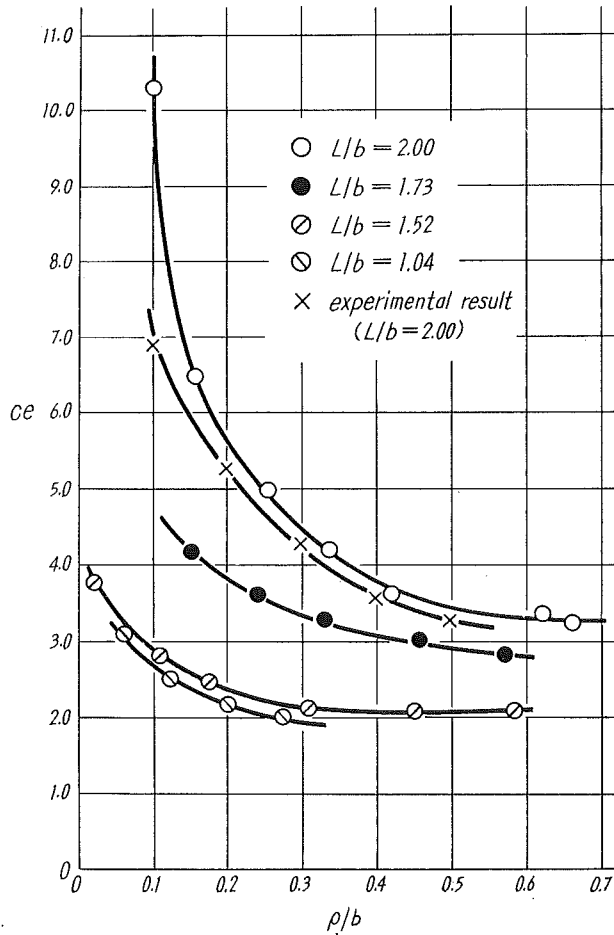

Fig. 14. (+)

α_0	α_1							α_2	α_3	L/b
1°	5°	10°	15°	20°	25°	30°	40°	$90° - \alpha_1$	89°	2.00
2°	5°	10°	15°	20°	25°			$90° - \alpha_1$	88°	1.73
3°	5°	10°	15°	20°	25°	30°	40°	$90° - \alpha_1$	87°	1.52
15°	20°	25°	30°	35°				$90° - \alpha_1$	75°	1.04

The values of stress-concentration factor for $L/b = 1.5$ and 1.04 are nearly the same. This means also that for large leg-thickness the configuration of +-section approaches the square and so the values of Ce approach the constant value at a comparatively small value of ρ/b. This shows an effective influence of the leg-length, thickness and fillet radius on the stress-concentration factor because of the decrease of the constant thickness zone rather than the increase of the leg-length.

For the case of the ratio $L/b = 1.73$, the stress-concentration factor is much higher than the previous two cases (i. e., $L/b = 1.52$ and 1.04).

For the case of the ratio $L/b = 2.0$, the ratios ρ/b have a more distinct influence on the value of the stress-concentration factor. The experimental results for theratio L/b of 2.0 are also shown in Fig. 14. Very little work has been done on the stress concentration in the +-section. As far as the authors know, only Beadle and Conway calculated values by using the same

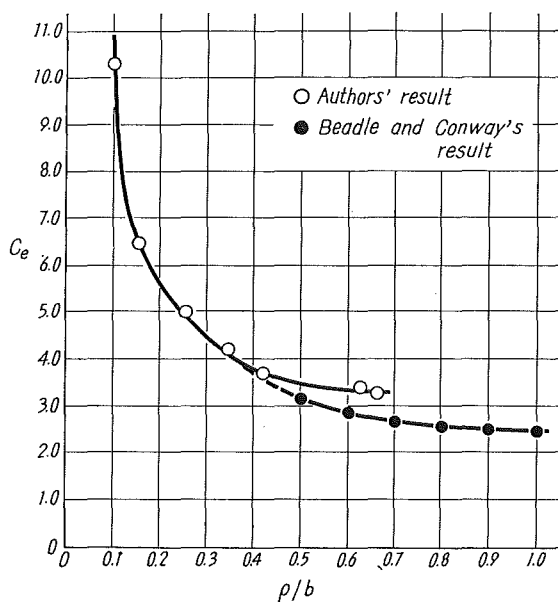Fig. 15. (+)

assumptions and method as for the T-section. Their results are for ratios ρ/b greater than 0.5. Fig. 15 shows their results together with that of the authors. From Fig. 15, we can see that two curves appear to coincide near the value of $\rho/b=0.5$. Then it may be considered that for the case of $L/b=2.0$ the stress-concentration is independent of the leg-lemgth, thickness and fillet radius.

7. Conclusions.

(1) The torsion problem of prismatical bars with L, T and cruciform-sections is investigated by means of the Schwarz-Christoffel transformation. The effects of the leg-length, -thickness and fillet radius are considered. Mapping the cross-section of the bars in the z-plane on to the unit circles in the ζ-plane and using a digital computer, the torsion stresses and the values of the stress-concentration factors for these shapes of section are calculated.

(2) Concerning the L-section with the value of L/b nearly equal to 2.0, the stress-concentration factor approaches a constant value with the decrease of the constant-thickness zone for a large fillet radius, and as the configuration of the section becomes a square with the increase of the leg-thickness for a constant fillet radius. Theoretical results agree satisfactorily with the experimental results utilizing the conducting-sheet analogy.

(3) Concerning the T-section, with the values of $w/b=1.0$, 0.925. and 0.902 i. e. $L/b=1.72$, 1.31 and 1.92 respectively, the stress-concentration factors for previous two cases are almost the same and approach a constant value at a comparatively small value of ρ/b, due to their large leg- (or web-) thickness.

For the case of $w/b=0.902$ (i. e. $L/b=1.92$), the stress concentration factor is higher than the previous two cases and is clearly influenced by the fillet radius.

The theoretical results are also in reasonable agreement with the experimental results.

(4) Concerning the cruciform-section with the values of $L/b=1.52$ and 1.04, the values of the stress-concentration factor are about the same and show the same inclination as for the T-section, that is, these values approach a constant value at a comparatively small fillet radius, due to their large leg-thickness; but the rate of change with the value of ρ/b is not large. On the other hand, for the cases of $L/b=2.0$, 1.73 the values of stress-concentration factor are clearly influenced by the fillet radius and their rates of change are larger than the former two cases. The curve of Ce against ρ/b for L/b of 2.00 has good connection with the curve obtained by Beadle and Conway.

Theoretical results agree reasonably with the experimental results.

(5)   Finally, it is found that the values of the stress-concentration factor for the **L, T** and cruciform-sections with various proportions are obtained only by changing the angles of α_n $(\alpha_0, \alpha_1, \alpha_2, \alpha_3)$.

Bibliographies

1)   Muskhelishvili: Some Basic Problems of Mathemalical Theory of Elasticity (1953), 571.
2)   A. R. Forsyth: Theory of Function of Complex Variable (1965), Vol. 2, 678.
3)   Y. Nomura: Transactions of the JSME, 25 (1959), 1048.
4)   N. S. Waner and W. W. Soroka: Proc. Soc. for Experimental Stress Analysis, 11 (1953), 19.
5)   Timoshenko: Theory of Elasticity (Second Edition), 288.
6)   J. H. Huth: Journ. Appl. Mech., 12 (1950), 388.
7)   E. Trefftz: Z. A. M. M. 82 (1921), 97.
8)   H. Nakazawa: Transaction of the JSME, 20 (1954), 444.
9)   C. W. Bealde and H. D. Conway: Transaction of ASME, Journ. Appl. Mech. 30 (1963), 138,